The versatility of collimated plane grating monochromators

Rolf Follath*

BESSY GmbH EXP, Albert-Einstein-Str. 15, D-12489 Berlin, Germany

Abstract

In the last few years monochromator development at the German synchrotron radiation facility BESSY II improved conventional monochromator designs, especially the SX700 design, considerably. It was possible to convert the high brilliance of undulator radiation at third generation synchrotron sources very successfully into outstanding monochromator performance in terms of high energy resolution, photon flux and focus size. New mechanical designs and precise control of the angular settings of optical elements resulted in very high monochromator stability and allowed even for an absolute energy calibration of monochromators. This report reviews the design principles of collimated plane grating monochromators and presents results obtained within the first two years of BESSY II operation. © 2001 Elsevier Science B.V. All rights reserved.

1. Introduction

Within the last 40 years a wide variety of beamline designs have been developed to meet the requirements of new and more sophisticated experiments. Although their designs follow different evolutionary paths, all of them had to address at least some of the following subjects.

- high energy resolution;
- high (spectral) flux and high (spectral) flux density;
- high spectral purity;
- large spectral range;
- accurate energy calibration.

Of course these requirements can not be fulfilled simultaneously and usually not even alternatively within one monochromator design. But the situation improved considerably with the installation of monochromators with variable deviation angle.

The development of these monochromators started with the GLEISPIEMO [1], led over the SX700 [2,12] and the SGM with variable included angle [3] (FSGM for focusing SGM) to the modern high performance monochromators installed at 3rd and 4th generation synchrotron sources [4].

The variable included angle design takes advantage of the ambiguity in the grating equation

$$Nk\lambda = \sin\alpha + \sin\beta \tag{1}$$

(N: line density, k: diffraction order). Within the working range of a monochromator, a given

*Tel.: +49-030-6392-4865; fax: +49-030-6392-4865.
E-mail address:* follath@bessy.de (R. Follath).

wavelength λ can be obtained by an almost arbitrary choice of the incidence and diffraction angles α and β (here measured to the normal). This degree of freedom is utilised in the FSGM to fulfill the focusing condition for spherical gratings not only at two energy positions as in the former SGMs and TGMs but within a wide energy range [5]. In the final design of the beamline however, this degree of freedom is fixed to the focusing curve and cannot be altered any more.

PGMs allocate dispersing and focusing properties to seperate optical elements. In principle they beware the degree of freedom in the grating equation even when the beamlines are completed. It was 1981 when Petersen [2] became aware that synchrotron radiation, although emitted in a narrow cone, cannot be treated as collimated light and the focusing properties of the plane grating operated in divergent light [6] have to be accounted for.

A source with size S in a distance r from the grating is imaged to a virtual source with size $S' = cS$ at a distance $r' = -c^2 r$ behind the grating. The ratio

$$c = \frac{\cos \beta}{\cos \alpha} \qquad (2)$$

is herein called the fix focus constant. As in the case of the FSGM, the focusing properties of the plane grating requires the fulfillment of a focusing condition (c = const. for plane gratings) within the whole energy range. The angular divergence $\Delta\alpha$ and beam cross sections b are additionally changed according to

$$\Delta\alpha' = \Delta\alpha/c$$
$$b' = bc. \qquad (3)$$

The limitations of Eq. (2) can be overcome when the plane grating is really operated in collimated light. In that case the PGM preserves the degree of freedom in the grating equation even for the completed and operating beamline.

2. Design principles of collimated PGMs

The optical design (Fig. 1) of the U125/1-PGMs takes the pattern for all of our collimated PGMs. Up to now a total number of 8 beamlines of similar designs are in operation at BESSY II (Table 1). Their main design features are

- sagittal focusing with horizontal deflection for collimation and focusing;
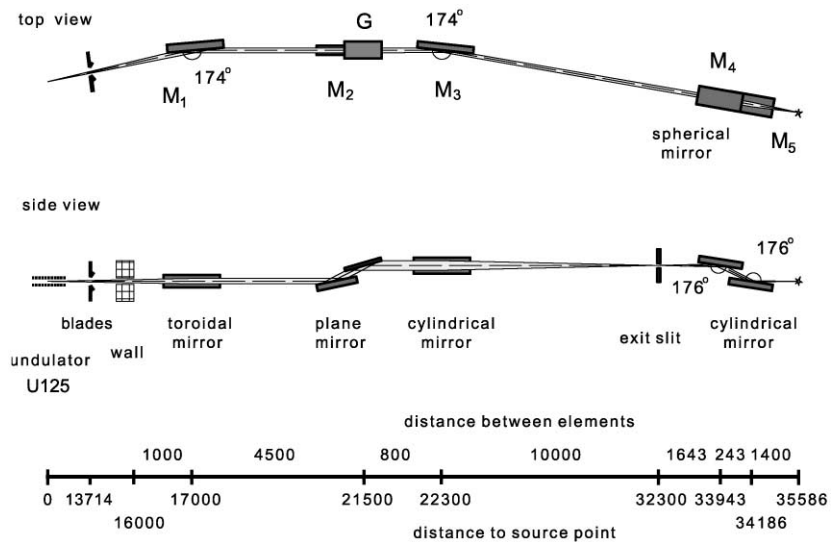

Fig. 1. Optical design of the U125/1-PGM. This monochromator was the first collimated PGM installed at BESSY II.

Table 1
Operational collimated plane grating monochromators at BESSY II

Beamline	Energy range (eV)	Resolving power	Dedication
U125/1-PGM	15–600	100.000[a]	low energy beamline
UE56/1-PGM	60–1500	100.000[a]	circularly polarised, two chopped beams
UE56/2-PGM1	”	110.000[a]	”
UE56/2-PGM2	”	110.000[a]	”
U41-PGM	170–2000	6.000[b]	high energy, high flux, small focus
U49/1-PGM	130–2000	10.000[b]	PEEM
U49/2-PGM2	80–2000	10.000[b]	PEEM
U180-PGM	30–1900[c]	30.000[a]	reflectometry, high spectral purity

[a] Aligned and determined with helium $(2 - 1_3)$-profile.
[b] Aligned and determined with $N_2 : 1s \rightarrow \pi^*$ core hole absorption.
[c] Wiggler mode of the insertion device.

Table 2
Comparison of focus sizes between meridional and sagittal focusing configurations

Slope error	Sagittal focusing Size (hor. × vert.) (μm^2)	Area (μm^2)	Meridional focusing Size (hor. × vert.) (μm^2)	Area (μm^2)
0.1″	300 × 20	6000	300 × 26	7800
1″	345 × 22	7590	300 × 171	51300

- variable deviation angle with an SX700 mount of the plane mirror [7,8];
- use of vertically collimated light for free choice of the focus constant c;
- collimation or moderate horizontal focusing by means of the first mirror;
- large focal lengths of 17 and 10 m, respectively to keep the optical abberations small;
- a switching of M_1 allows for a second beamline sharing the same undulator source.

2.1. Sagittal focusing

Although sagittal focusing is known for a long time [9], it is very impressive to illustrate this method with an application at a synchrotron radiation source. For that we compare a meridional and sagittal 1 : 1 imaging with a single mirror at a high beta section of BESSY II as in the UE56/1-PGM design [10]. The sigma values of horizontal and vertical source sizes are 300 and 20 μm, respectively. For clarity we neglect optical abberations in this example. We find that even with very good optical elements of 0.1″ meridional focusing with a vertically deflecting mirror increases the image size by 30% whereas sagittal focusing with a horizontally deflecting mirror preserves the size and thus the brilliance. The difference becomes more drastic when the slope errors are increased to 1″. In that case the meridional focusing increases the image size by nearly one order of magnitude compared to 25% for the sagittal focusing. The results are summarised in Table 2. This demonstrates that the benefit of sagittal focusing increases under bad conditions e.g. surface distortions caused by high heat loads. Unfortunately, the advantage of sagittal focusing is partly cancelled by the fact that usually the short sagittal radius is not as perfect as the long meridional one. But even if we

compare a sagittal focusing with $1''$ slope error to a meridional with $0.1''$ its advantage is still obvious.

2.2. Accessible parameter space

The energy E and c-parameter space accessible for a monochromator is shown in Fig. 2. It is confined by the mechanical limits of the rotation angles for plane mirror (θ) and grating (β) and the geometrical size of the plane mirror. In inside diffraction order ($c > 1$) the accessible energy range for the commonly used c-value of 2 is 15–600 eV for a grating with 300 lines/mm. In outside diffraction order the lowest energy is 5.5 eV limited by the minimum value of $\theta = 79°$. The energy resolution of grazing incidence PGMs operating with fixed c-value scales like $1/\sqrt{E}$ compared to $1/E$ for FSGMs. PGMs therefore offer high performance over a large spectral range with a single grating. The solid lines in Fig. 2 show focal curves for on-blaze modes with blaze angles of $1°$, $2°$ and $3°$, respectively. A grating with $2°$ blaze angle can operate on blaze between 30 and 160 eV.

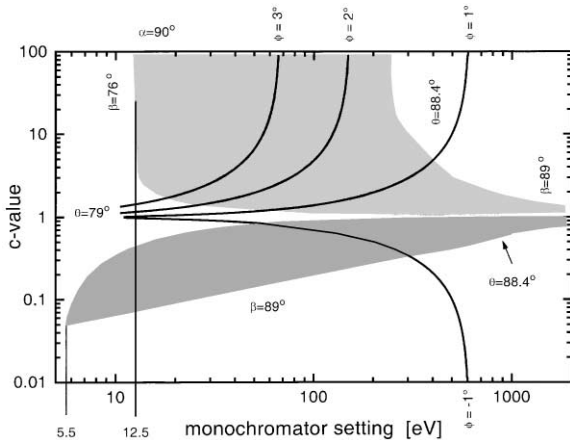PGMs are commonly designed for inside diffraction order. The mechanics offer then a large

parameter range for $c > 1$. Against that, monochromators optimised for high flux densities are usually operated in outside diffraction order like the U41-PGM at BESSY II [11]. For that purpose it is advantageous to rotate the complete grating chamber around its vertical axis and place the grating in front of the plane mirror. For reasons shown in the next section this improves also the influence of slope errors of the plane mirror to the performance of the beamline.

2.3. Contributions of slope errors

The contributions of slope and figure errors of optical elements to the resolving power change with c-value. This behaviour can be approximated for the grazing incidence regime as described in [4]. Fig. 3 shows this behaviour for optical elements
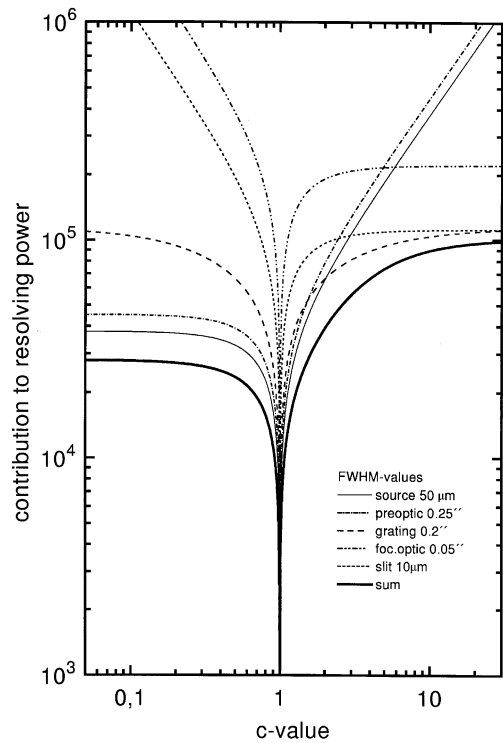

Fig. 3. Contributions of source size and effective slope and figure errors of optical elements to the resolving power. Data are taken from optical elements as inserted in the U125/1-PGM and calculated for 60 eV.

Fig. 2. (E, c)-parameter space of the U125/1-PGM for the 300 lines/mm grating. The mechanical limits are $\theta \in [79°, 90°]$, $\beta \in [-76°, -89°]$. The length of the plane mirror sets a limit to $\theta < 88.4°$. Solid lines represent on-blaze curves for gratings with $-1°, 1°, 2°$ and $3°$, respectively.

with surface qualities as inserted in the U125/1-PGM. In inside diffraction order the resolving power is limited by source size and slope errors of the preoptic for $c \leqslant 2$. Above this value the grating limits the performance. But this limit increases with increasing c-value because the effective slope error of the grating σ'_{gr} scales like $\sigma'_{gr} = \sigma_{gr}(1 + c)/(2c)$. Its value can come down to $\sigma_{gr}/2$ for very large c-values where the focusing mirror is the resolution limiting element. The contribution of the focusing mirror is not affected by the c-variation. Here we take advantage of the sagittal focusing which reduces the slope errors by a factor of 20 for a deflection angle of $3°$. The residual variation of this contribution is due to the change in dispersion, which is shown for a 10 μm exit slit setting.

In outside diffraction order $c < 1$ the resolving power is entirely limited by the source size and the slope errors of the preoptic. This is due to the angular magnification (Eq. (3)) and manifests itself by an increase of preoptic slope errors σ_{po} to an effective slope error according to $\sigma'_{po} = \sigma_{po}/c$. Monochromators designed for $c < 1$ should therefore place the plane mirror behind the grating.

The absorption profile of the $N_2 : 1s \rightarrow \pi^*$-transition is frequently used to determine the resolving power of monochromators. We recorded the spectrum and fitted a set of nine Voigt profiles with equal widths to the data. The Gaussian contribution of the profile is usually attributed to the monochromator, whereas the Lorentzian is taken as the natural line width. We found a Lorentzian width of 113 ± 1 meV and a Gaussian width between 35 ± 1 meV at the U125/1-PGM and 20 meV at the UE56/1-PGM. The Lorentzian width is in good agreement to other measurements [14], which may indicate that this is really the natural linewidth of this transition.

The difficulties one encounteres in the numerical treatment of the spectrum show that it is not suitable to proof the ultimate resolving power of high performance beamlines. A more appropriate system for that purpose is the autoionisation process of doubly excited helium, especially the $(2, -1_3)$-profile within one of its Rydberg series. This line has a predicted natural linewidth of only 3 μeV [15], which is Doppler broadened to 400 μeV at room temperature. Beamlines that cover the photon energy of 64 eV should be
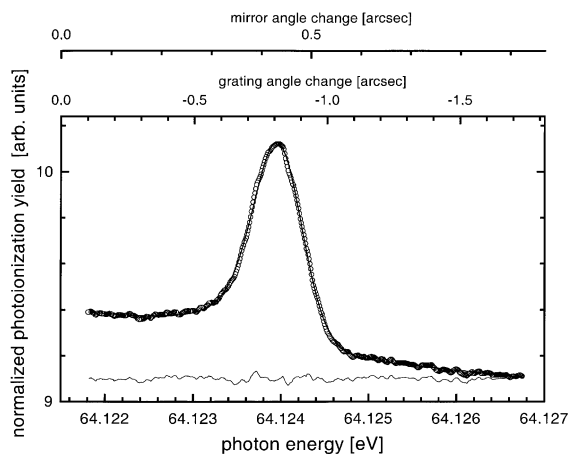
3. Performance of collimated PGMs

3.1. Resolving power

The final alignment of the monochromators was performed by optimising their energy resolution as determined by total ionisation yield measurements of various gases. The measurements were performed by means of an ionisation chamber integrated in the beamline between exit slit and refocusing optics. It turned out that this integrated chamber is very useful to check and maintain the beamline performance. Reviews of resolving power and energy calibration can be performed within half an hour. The ability to record absorption spectras with different c-values allows even for a rapid restoration of the absolute energy scale of the monochromator which might become necessary after a grating change or drifts in the source position [13].

Fig. 4. $(2, -1_3)$-resonance of doubly excited helium taken at the UE56/2-PGM2. Points: experimental data; upper full curve: fit of a Fano profile convoluted with a Gauss profile; lower full curve: residual of the fit.

optimised with the help of this profile. Fig. 4 shows the profile measured with the beamline UE56/2-PGM2. The total linewidth was found to be 690 μeV. If we allow for the Doppler contribution this gives a monochromator bandwidth of 560 μeV which corresponds to a resolving power of 110 000. The monochromator stepwidth was only 10 μeV and corresponds to a grating rotation of 17 nrad and a plane mirror rotation of only 9 nrad. An overview of the resolving powers of the collimated PGMs at BESSY II is given in Table 2, five of them could be optimised with the help of the helium resonance, three of them with the $N_2 : 1s \rightarrow \pi^*$-spectrum.

Fig. 5. Flux measurements at the U125/1-PGM with the 300 lines/mm-grating at an exit slit width of 100 μm. The c-values are 2.25 for the thin curve and 1.4 for the thick curve, respectively. The photon numbers are calculated by dividing the measured photocurrent of a GaAsP photodiode by the quantum efficiency of the detector. The dashed line shows a monochromator scan with fixed undulator gap.

3.2. Flux and high order suppression

The flux measurements were made in the coupled mode, where undulator and monochromator are scanned in parallel. This allows the monochromator to stay on top of the undulator harmonic, while scanning over the desired energy range. Fig. 5 shows the flux in the first, third and fifth harmonic of the low energy beamline U125/1-PGM. For the corresponding data of the UE56/1-PGM and U41-PGM see [16,17]. With an exit slit width setting of 100 μm the photon flux is around 10^{13} 1/s for the first undulator harmonic. Taking dispersion into account, the spectral flux density is well above 10^{13} 1/(s × 0.1% BW). All flux curves show characteristic absorption minima at 284 eV (carbon) and 540 eV (oxygen). They are caused by contaminations of the optical surfaces and the surface of the GaAsP photodiode. The surface quality of the optical elements can be restored by a cleaning method [18].

The flux curves obtained with $c = 1.4$ show significant drops in the energy range between 200 and 400 eV. This is due to the minimum in the grating efficiency and already predicted by theoretical calculations [19]. From Fig. 5 it is obvious, that the utilisation of this property can—at least in some energy ranges—double the photon flux compared to an operation with fixed c-value.

Besides high flux values, the spectral purity of the delivered synchrotron light is of crucial importance for experiments. The suppression of the high order light is therefore an important subject. However, systematic quantitative measurements of higher order contributions are extensive and require a well characterised secondary monochromator at the end of the beamline [20]. A quicker, qualitative analysis of the higher orders can be done utilising the line structure of the undulator radiation. The emitted undulator radiation consists of equidistant lines at multiples of the fundamental undulator harmonic energy. They appear in higher diffraction orders at the end of the beamline and can be suppressed by an appropriated choice of the c-value as shown in Fig. 6. The measurement with $c = 2.25$ shows clearly the peak of false light at 200 eV. Although the monochromator setting suggests an energy of
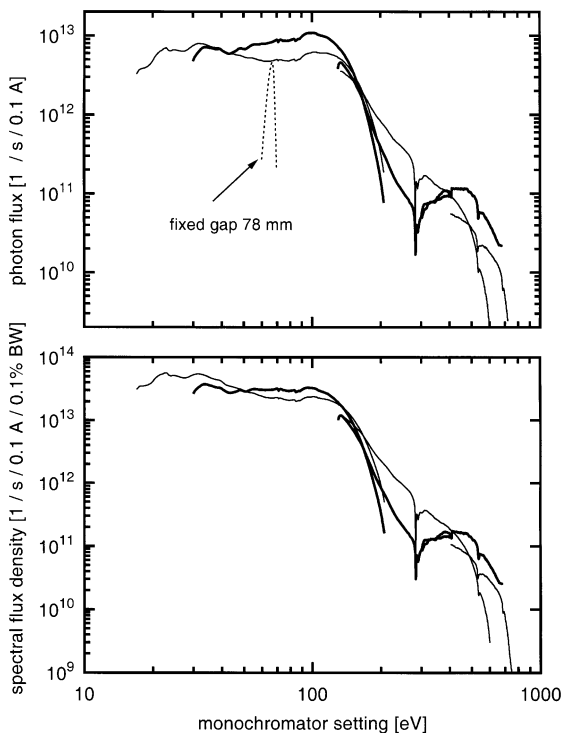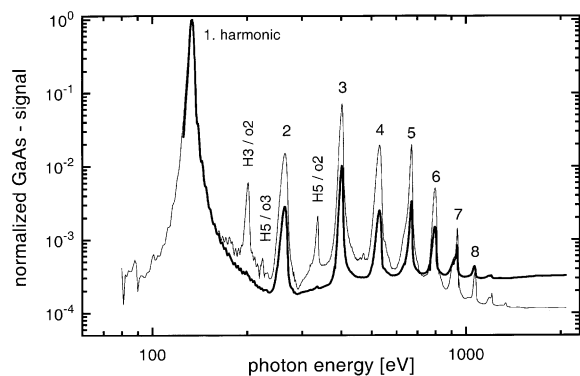
Fig. 6. Undulator spectrum with fixed gap of 101 mm ($k = 1.3$) obtained with $c = 2.25$ (thin line) and $c = 1.4$ (thick line). The fundamental appears at 135 eV. Higher order contributions of the grating (H3/o2), (H5/o2) and (H5/o3) vanish for $c = 1.4$ (H: undulator harmonic, o: order of diffraction.

200 eV, this light originates mainly in the 2. diffraction order of the 3. undulator harmonic and has therefore an energy of 400 eV. The small wiggles between the first and second order are an attribute of the undulator and no false light, their number is related to the number of undulator periods. The operation with $c = 1.4$ eliminates the higher order contributions at 200 eV completely and—if the fundamental of the undulator is set to 200 eV—delivers light of high spectral purity. However, because the c-value of 1.4 is nearer to the zero order (zero order would have $c = 1$), the background of stray light at high energies is much higher than for $c = 2.25$.

At lower energies and higher k-values of the undulator the spectrum gets more complex and the suppression is more difficult. This is mainly due to the restricted deviation angle ($2\theta_{min} = 158°$ in our designs) and common to all grazing incidence monochromators. In the low energy range the use of filters for high order suppression is therefore unavoidable.

3.3. Focus size

The size of the focus is mainly determined by the refocusing optics. Large demagnifications require short focal distances, whereas at least some experiments need free space for e.g. differential pumping systems. The beamline design has

therefore to balance between focus size and geometrical distance between last focusing element and axial focus position. For small spot sizes with very high flux densities, the monochromator must be optimised in a manner that the total flux through a given small exit slit width is maximised [17]. This is achieved by maximising the spectral bandwidth of the monochromator, using blazed gratings with low line densities in outside diffraction order. The collimated design allows herein the maintainance of the on-blaze condition over a large energy range [11].

4. Conclusion

The collimated PGM offers an easy to handle beamline design for a wide variety of experimental requirements. Its versatility makes it ideally suitable for general purpose beamlines with frequently changing experimental stations. The beam characteristics like divergence, energy bandwidth or spectral purity can easily be adapted to specific experimental demands by changing a single value in the computer control system. Up to now a total number of 8 insertion device beamlines of this type are in successful operation at BESSY II and five additionals are currently under construction.

References

[1] C. Kunz et al., J. Opt. Soc. Am. 58 (1968) 1415.
[2] H. Petersen, Opt. Comm. 40 (1982) 402.
[3] W.B. Peatman et al., Rev. Sci. Instrum. 66 (1995) 2801.
[4] R. Follath, F. Senf, Nucl. Instr. and Meth. A 390 (1997) 388.
[5] H.A. Padmore, Rev. Sci. Instrum. 60 (1988) 1608.
[6] M. Murty, J. Opt. Soc. Am. 52 (1962) 768.
[7] F. Riemer, R. Torge, Nucl. Instr. and Meth. 208 (1983) 313.
[8] A.V. Pimpale, S.K. Deshpande, V.G. Bhide, Appl. Opt. 30 (1991) 1591.
[9] W. Cash, Appl. Optics 26 (1987) 2915.
[10] K.J.S. Sawhney et al., Nucl. Instr. and Meth. A 390 (1997) 395.
[11] M.R. Weiss, R. Follath, F. Senf, W. Gudat, J. Electr. Spectr. Rel. Phenom. 101 (1999) 1003.
[12] H. Petersen, Rev. Sci. Instrum. 66 (1995) 1.
[13] M. Weiss, R. Follath, K.J.S. Sahwney, T. Zescke, Nucl. Instr. and Meth. A 467–468 (2001), this proceedings.

[14] K.C. Prince et al., J. Electr. Spectr. Rel. Phenom. 101 (1999) 141.

[15] J.M. Rost et al., J. Phys. B 30 (1997) 4663.

[16] M. Weiss et al., Nucl. Instr. and Meth. A 467–468 (2001), this proceedings.

[17] C. Jung et al., Nucl. Instr. and Meth. A 467–468 (2001), this proceedings.

[18] F. Eggenstein et al., Nucl. Instr. and Meth. A 467–468 (2001), this proceedings.

[19] R. Follath, F. Senf, W. Gudat, J. Synchrotr. Rad. 5 (1998) 769.

[20] F. Scholze et al., Nucl. Instr. and Meth. A 467–468 (2001), this proceedings.